Cell Cycle Checkpoints, DNA Damage/Repair, and Lung Cancer Risk

Xifeng Wu,[1] Jack A. Roth,[2] Hua Zhao,[1] Sherry Luo,[1] Yun-Ling Zheng,[3] Silvia Chiang,[1] and Margaret R. Spitz[1]

Departments of [1]Epidemiology and [2]Thoracic & Cardiovascular Surgery, University of Texas M.D. Anderson Cancer Center, Houston, Texas and [3]Cancer Genetics and Epidemiology Program, Lombardi Cancer Center, Georgetown University Medical Center, Washington, District of Columbia

Abstract

Given that defects in cell cycle control and DNA repair capacity may contribute to tumorigenesis, we hypothesized that patients with lung cancer would be more likely than healthy controls to exhibit deficiencies in cell cycle checkpoints and/or DNA repair capacity as gauged by cellular response to *in vitro* carcinogen exposure. In an ongoing case-control study of 155 patients with newly diagnosed lung cancer and 153 healthy controls, we used the comet assay to investigate the roles of cell cycle checkpoints and DNA damage/repair capability in lung tumorigenesis. The median γ-radiation-induced and benzo(*a*)pyrene diol epoxide–induced Olive tail moments, the comet assay parameter for measuring DNA damage, were significantly higher in the case group (5.31 and 4.22, respectively) than in the control group (4.42 and 2.83, respectively; $P < 0.001$). Higher tail moments of γ-radiation and benzo(*a*)pyrene diol epoxide–induced comets were significantly associated with 2.32- and 4.49-fold elevated risks, respectively, of lung cancer. The median γ-radiation-induced increases of cells in the S and G_2 phases were significantly lower in cases (22.2% and 12.2%, respectively) than in controls (31.1% and 14.9%, respectively; $P < 0.001$). Shorter durations of the S and G_2 phases resulted in 4.54- and 1.85-fold increased risks, respectively, of lung cancer. Also observed were joint effects between γ-radiation-induced increases of S and G_2 phase frequencies and mutagen-induced comets. In addition, we found that in controls, the S phase decreased as tail moment increased. This study is significant because it provides the first molecular epidemiologic evidence linking defects in cell cycle checkpoints and DNA damage/repair capacity to elevated lung cancer risk. (Cancer Res 2005; 65(1): 349-57)

Introduction

As exogenous and endogenous agents continuously bombard DNA, a complex, highly preserved, and well-regulated system routinely checks for and repairs the resulting damage. Depending on the type of damage sustained, cells undergo three different types of DNA repair. When lesions are simple, repair occurs quickly without affecting cell division. When lesions are complex, the local response, which entails the recruitment of additional factors, provides the first-line defense. Failure of the local response to fully repair the lesion then activates the DNA damage response, also known as the global response. Although the intricacies of the global response have not yet been fully elucidated, processes such as chromatin modulation, posttranslational modification of the proteins involved in DNA repair mechanisms, up-regulation of the DNA repair capacity, and changes in cell cycle progression are thought to be involved (1).

It is widely accepted that there is substantial interindividual variation in DNA repair capacity. In an extensive review of the literature on DNA repair and susceptibility to cancer in humans, Berwick and Vineis conclude that most studies show a difference between cancer case subjects and control subjects" (2). Mutagen sensitivity and host cell reactivation assays have reinforced the association between suboptimal DNA repair capacity and genomic instability and, hence, an increased cancer risk (3–5). The comet assay is advantageous to other methods of DNA damage/repair detection because it is efficient, can detect minimal DNA damage using just a small number of cells, has potential for high throughput, and has high reproducibility (6). Numerous cancer studies, including those by Rajeswari et al. (7), Colleu-Durel et al. (8), Rajaee-Behbahani et al. (9), and Kleinsasser et al. (10), have used the comet assay to show case-control differences in baseline and induced DNA damage using a variety of test mutagens.

Cell cycle checkpoints are biochemical signaling pathways that sense damage to the DNA structure or impaired chromosome function and elicit complex cellular repair responses. These checkpoints rapidly induce cell cycle delay, generally at the G_1, S, and G_2 checkpoints, allowing time for the activation of DNA repair mechanisms. The checkpoints also maintain cell cycle arrest while the repair takes place and initiate cell cycle progression once repair is complete (11). If the DNA cannot be repaired adequately, the cell then undergoes permanent cell cycle arrest and apoptosis. Incorrectly repaired DNA, however, continues to replicate, leading to accumulation of the mutation and, thus, elevated cancer risk. Studies have shown that mutations in cell cycle control genes, such as *p53* and *p21*, are directly linked to chromosomal aberrations and genomic instability (12). In addition, patients with ataxia-telangiectasia syndrome and Nijmegen breakage syndrome, who have defects in DNA damage checkpoints, have been found to be hypersensitive to ionizing radiation (13). These examples from recent literature illustrate the cause-effect relationship between defects in checkpoints and the accumulation of chromosomal aberrations and subsequent increased cancer risk (11).

We have applied molecular epidemiologic principles and modified assays to assess cell cycle checkpoints and DNA damage/repair in patients with lung cancer and healthy controls. We used a fluorescence-activated cell-sorting (FACS) method to examine cell cycle checkpoints and the alkaline comet assay to measure DNA damage/repair. By using the comet assay we measured the net result of DNA damage/repair. By selecting challenge mutagens to induce specific types of DNA damage, we were able to evaluate host susceptibility for particular DNA repair pathways. For example, γ-radiation, a mutagen capable of

Requests for reprints: Xifeng Wu, Department of Epidemiology, Box 189, University of Texas M.D. Anderson Cancer Center, 1515 Holcombe Boulevard, Houston, TX 77030. Phone: 713-745-2485; Fax: 713-792-0807; E-mail: xwu@mdanderson.org.

*I*2005 American Association for Cancer Research.

inducing single- and double-strand breaks, activates cell cycle checkpoint and initiates base excision repair and/or double-strand break repair. Therefore, exposure to γ-radiation allows assessment of base excision repair and double-strand break, the pathways that this particular mutagen triggers. In contrast, benzo(*a*)pyrene diol epoxide (BPDE), a metabolite product of the tobacco smoke procarcinogen benzo(*a*)pyrene, forms DNA adducts *in vivo* and *in vitro*, activating nucleotide excision repair. Using BPDE and γ-radiation in parallel, we were able to measure different DNA repair pathways. Furthermore, because γ-radiation-induced cell cycle arrest provides more time for cellular DNA damage repair, individuals with defects in one or more of these DNA repair systems or cell cycle checkpoints may exhibit greater sensitivity to the relevant mutagen challenge that translates to greater risk of cancer. We therefore hypothesized that deficiencies in cell cycle checkpoints and/or DNA repair capacity following exposure to γ-radiation would be more apparent in patients with lung cancer than in control subjects.

Materials and Methods

Study Population. One hundred fifty-five patients with newly diagnosed, histologically confirmed lung cancer were consecutively recruited from the University of Texas M.D. Anderson Cancer Center in Houston, Texas. Approximately 20% of the cases refused or were too ill to participate. To identify prospective study participants, M.D. Anderson staff interviewers review computerized daily appointment schedules for the thoracic medical and surgery clinics, where patients with lung cancer receive treatment. Each new patient is asked to complete a brief eligibility questionnaire that assesses prior cancer therapy, smoking status, and willingness to participate in the epidemiologic study. We enrolled all patients undergoing surgery, regardless of smoking status, and other select subgroups, including never smokers, ethnic minorities, and young patients.

Healthy controls with no prior history of cancer, except nonmelanoma skin cancer, were recruited on a voluntary basis from the Kelsey-Seybold clinics, the largest multispecialty physician group in the Houston metropolitan area. The response rate for participation of these controls was 73.3%. The controls were frequency matched to the cases with a 1:1 ratio by age, sex, and ethnicity. Because the study is ongoing, perfect matching has not yet been achieved. A total of 153 control subjects have been included for this study. The process we implemented in identifying and recruiting control subjects is described in detail in Hudmon et al. (14).

Epidemiologic Data. At the start of the interview, M.D. Anderson staff members briefly explained the premise of the study to the participant and obtained the signed informed consent form approved by the M.D. Anderson and Kelsey-Seybold Institutional Review Boards. During the interview, information about demographics, smoking history, alcohol consumption, family history of cancer, medical history, and occupational history was collected. At the conclusion of the interview, 40 mL of blood were drawn from each participant into coded heparinized tubes.

Tissue Cultures. Blood cultures were prepared immediately after the samples were delivered to the laboratory. Laboratory technicians were blinded to the case-control status. Phytohemagglutinin antigen–stimulated cultures (Wellcome Research Laboratories, Research Triangle Park, NC) were established in 60 × 15-mm Petri dishes (Falcon, Franklin, NJ) using 0.4 mL of the fresh peripheral blood sample with 1.6 mL of RPMI 1640 (Life Technologies, Inc., Rockville, MD) and supplemented with 15% fetal bovine serum (Life Technologies). Separate blood cultures for baseline and mutagen-induced comets were established for each study subject 96 hours prior to the comet assay. For the BPDE treatment, a final concentration of 2 μmol/L BPDE (10 μL of 0.4 mmol/L BPDE in 2 mL of blood medium) were added 24 hours prior to the comet assay. For the γ-radiation treatment, cells were exposed to 1.5-Gy γ-radiation from a cesium-137 source (cesium irradiator Mark 1, Model 30; J.L. Shepherd and Associates, Glendale, CA) at room temperature. Following γ-irradiation, blood cultures were placed on ice to minimize DNA repair, and the comet assay was done 15 minutes after radiation.

Comet Assay. In a previous report (15), we elaborated on the details of our alkaline comet assay procedure, used to quantify DNA damage/repair, which is based on the method by Singh et al. (16). Briefly, for both the baseline and the mutagen-exposed cultures, 50 μL of the blood culture were mixed with 150 μL of 0.5% low melting point agarose (Life Technologies) and layered on fully frosted microscope slides precoated with 1% agarose. After the mixture was allowed to solidify at 4°C for 10 minutes, a third layer of 0.5% low melting point agarose was placed on top of the cell suspension/low melting point agarose layer on a slide, covered with a new glass coverslip, and placed on a 4°C metal plate for an additional 10 minutes. Cells were then exposed for approximately 1 hour at 4°C to freshly prepared 1× lysis buffer (2.5 mol/L NaCl, 100 mmol/L EDTA, 1% sodium sarcosinate, 10 mmol/L Tris, adjusted to pH 10 with NaOH, and completed with 10% DMSO and 1% Triton prior to use). Following cell lysis, the slides were placed in a horizontal electrophoresis box without power and filled with freshly prepared alkali buffer (300 mmol/L NaOH, 1 mmol/L EDTA, pH >13) at 4°C to allow for DNA denaturation and unwinding and the exposure of the alkali-labile sites. Electrophoresis was carried out by a constant electric current of 295 to 300 mA for 23 minutes at 4°C. After electrophoresis, the slides were neutralized with three 5-minute washes in 0.4 mol/L Tris-HCl (pH 7.4). Finally, the slides were fixed in 100% methanol for 5 to 10 minutes and stored in the dark at room temperature until analysis.

In this study, we modified the comet assay to measure net DNA damage. In the BPDE experiments, the peripheral blood lymphocytes were treated once with BPDE and incubated for an additional 24 hours before the comet assay was done. During this 24-hour period, cells were continuously removing and repairing BPDE-induced DNA damage. Breaks would be only transiently present as cells repaired lesions by nucleotide excision, so that a high level of breaks in our study after a 24-hour incubation should reflect poor nucleotide excision repair. A similar argument could be made for γ-radiation-induced DNA damage. Approximately 50% of γ-radiation-induced DNA damage will be repaired within 15 minutes by the fast-repair component, which will be activated within 5 minutes after exposure to γ-radiation (17). It is reported that cells from patients with ataxia-telangiectasia have a reduced fast-repair component in both G_1- and G_2-phase cells that operates on DNA double-strand breaks and chromosomal breaks. In our approach, γ-radiation was done at room temperature. Cells were then placed on ice blocks to slow DNA repair, embedded in agarose, and attached to the slides approximately 15 minutes after γ-radiation. Consequently, γ-radiation-induced comet cells should reflect the net result of DNA damage and repair because the fast component of DNA repair was not inhibited.

Quantification of DNA Damage. Immediately prior to imaging, the slides were hydrated by exposure to fresh 0.4 mol/L Tris buffer (pH 7.4) for approximately 30 minutes, and the DNA was stained by a 1-minute exposure to a fresh solution of 0.4 mol/L Tris containing 300 μL of 10 mg/mL ethidium bromide. Tail moment, which has been used in molecular epidemiology to quantify DNA damage ever since Olive showed its effectiveness, was calculated by [(tail mean − head mean) × (tail % DNA/100)] for 50 cells (25 cells from each end of the slide) using the Komet 4.0.2 imaging software (Kinetic Imaging Ltd., Liverpool, United Kingdom; ref. 18). The average Olive tail moment was calculated for the baseline comets and the BPDE- and γ-radiation-induced comets in each study subject.

Cell Cycle Analysis. For the cell cycle analysis, two blood cultures were set up for each subject. In each culture, 1 mL of whole blood was cultured in 9 mL of RPMI 1640 tissue-culture medium (JRM Biosciences, Lenexa, KS) with 10% FCS and 0.2 mL of phytohemagglutinin. Using doses of 1 to 7.5 Gy and post-γ-radiation exposure times of 1 to 48 hours, we previously determined the optimal dose of γ-radiation for the cell cycle analysis in peripheral blood leukocytes to be 2.5 Gy; we also determined the optimal time after γ-radiation exposure to be 10 hours (19). After 67 hours of incubation, the cells underwent γ-irradiation from a cesium-137 source. The cell cultures were then incubated for another 10 hours before being harvested. Unirradiated samples were harvested at the same time. The harvested cells were centrifuged, washed twice with 2 mL of PBS, and fixed with ethanol. Then, using a FACScan (Becton Dickinson Immunocytometry Systems, San Jose, CA), cell cycle phases of the samples were analyzed. Immediately before

Table 1. Distribution of select characteristics in case patients and control subjects

Variables	Cases (n = 155)	Controls (n = 153)	P
Sex, n (%)			
Male	72 (46.5)	84 (54.9)	0.138
Female	83 (53.5)	69 (45.1)	
Ethnicity, n (%)			
Caucasian	105 (67.7)	92 (60.1)	
Hispanic	10 (6.5)	16 (10.5)	
African American	40 (25.8)	45 (29.4)	0.283
Smoking status, n (%)			
Never smoker	36 (23.2)	55 (36.2)	
Former smoker	37 (36.8)	59 (38.8)	
Current smoker	62 (40.0)	38 (25.0)	0.008
Age, median (range)	62 (35–81)	62 (27–86)	0.640
Pack-years, median (range)*	39 (1–120)	26 (0.05–90)	0.0004

NOTE: One control had missing smoking information.
*For ever smokers only.

analysis, cell suspensions were filtered through a 37-μm filter to remove debris, and DNA was stained by adding 1 mL of a solution containing 250 μg/mL propidium iodide and 5 mg/mL RNase in PBS to 0.2 mL of the cell suspension. A minimum of 2×10^4 cells was analyzed in each sample. Cell cycle phase distributions were determined using Lysis 2 software (Becton Dickinson Immunocytometry Systems), and the percentage of cells in each phase was determined using ModFit software (Topsfield, ME).

Statistical Analysis. All statistical analyses were done with the Intercooled Stata 7.0 statistical software package (College Station, TX). The χ^2 test was used to test for differences in categorical data (e.g., sex, ethnicity, and smoking status) between cases and controls. For nonnormally distributed continuous variables (e.g., age, pack-year, cell cycle arrest, and tail moments), the nonparametric Wilcoxon rank sum test was used. Mutagen-induced tail moments and γ-radiation-induced S and G_2 phase arrests were analyzed as both continuous and categorical variables. Mutagen-induced tail moments were further dichotomized at the 75th percentile value in the control group: "Low" was defined as <75th percentile value of the tail moment in controls, and "high" was defined as ≥75th percentile value of the tail moment in controls. γ-Radiation-induced S and G_2 phase arrests were dichotomized at the 25th percentile value in the control group. "Long" was defined as >25th percentile value of the percentage of the specific phase of cells in the controls and "short" was defined as ≤25th percentile value of the percentage of the specific phase of cells in the controls. Our selection of these two cutoff points was based on our a priori hypothesis that increased DNA damage and shorter cell cycle duration are associated with cancer risk. Also, by using these cutoff points, we could form comparable groups among the cases and controls to provide a stable estimate of cancer risk association with these two variables. We also did analyses by quartile distributions.

Spearman correlation coefficients were calculated to determine the correlations between variables. To assess the strength of the associations between lung cancer risk and the levels of mutagen-induced tail moments and γ-radiation-induced cell cycle S and G_2 arrest, we calculated odds ratios (OR) and their 95% confidence intervals (95% CI) using unconditional logistic regression analysis. Multivariate analysis was used to adjust for potential confounding by sex, age, ethnicity (Caucasian, African American, or Hispanic), and cigarette smoking status (never, former, or current). An ever smoker was defined as an individual who had smoked at least 100 cigarettes in his or her lifetime. Ever smokers included former smokers, current smokers, and recent quitters (quit within the previous year). For cases, a former smoker was defined as an individual who had quit smoking at least 1 year before receiving the lung cancer diagnosis. For controls, a former smoker was defined as an individual who had quit smoking at least 1 year before the interview. Tests for a linear trend were done using quartile levels as continuous variables. We also explored the possibility of interactions using the product of the two variables as an interaction term in the logistic regression model. All P values were two-sided, and associations were considered statistically significant at $P < 0.05$.

Results

The cases and controls were adequately matched in terms of age, sex, and ethnicity (Table 1). There were statistically significantly more current smokers in the case group (40.0%) than in the control

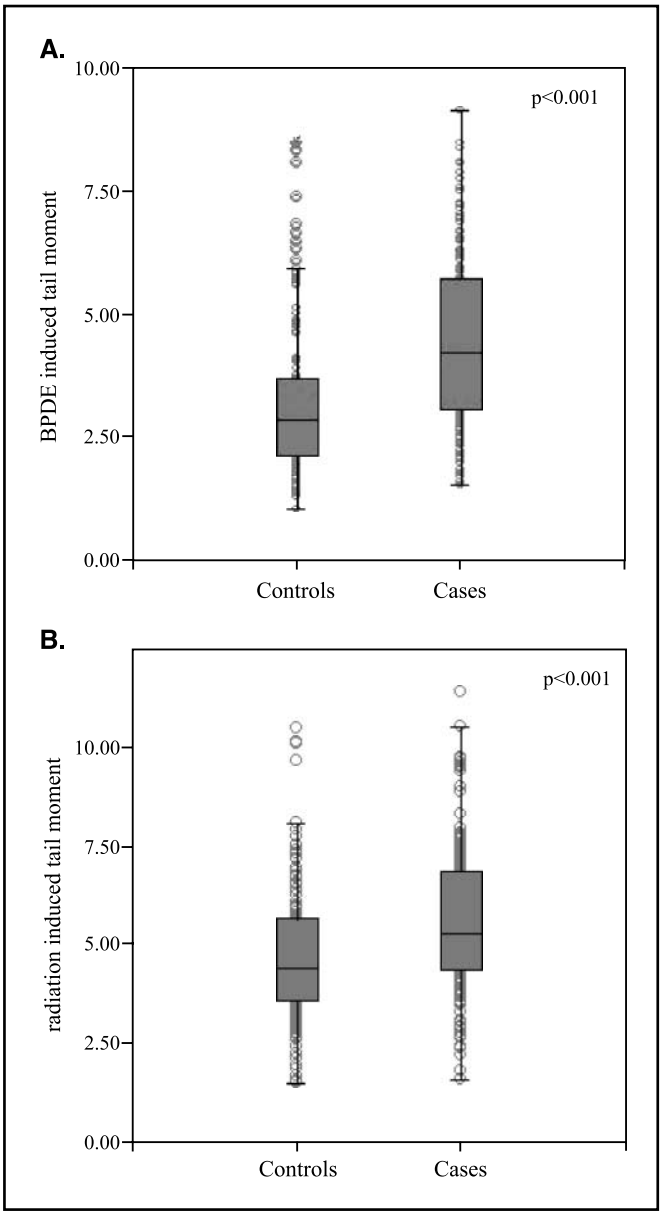

Figure 1. Frequency distribution of BPDE- and γ-radiation-induced tail moments in lung cancer cases and controls.

group (25.0%). Cases were also generally heavier smokers than controls (median pack-years, 39 versus 26; $P = 0.0004$).

The cases exhibited significantly higher levels of induced DNA damage than the controls (Fig. 1). Specifically, the median γ-radiation-induced (tail moments = 5.31 versus 4.42; $P = <0.001$) and BPDE-induced (tail moments = 4.22 versus 2.83; $P = <0.001$) levels of DNA damage were significantly higher in the cases than in the controls. When the study subjects were stratified by smoking status and γ-radiation-induced and BPDE-induced tail moments were compared between cases and controls, we found that median γ-radiation-induced and BPDE-induced tail moments were consistently significantly higher in cases than in controls across all three smoking-status groups, with the exception of γ-radiation-induced tail moment in former smokers, which conformed to the trend but not to statistical significance (data not shown). When the participants were stratified by case and control status and γ-radiation-induced and BPDE-induced tail moments were compared among never, former, and current smokers, we found that changes in γ-radiation-induced and BPDE-induced tail moment did not correlate with changes in smoking status in either cases or controls (data not shown), with the exception of BPDE-induced tail moment in controls. We also compared median γ-radiation-induced and BPDE-induced tail moments between ever smoker controls and never smoker cases and discovered that the median γ-radiation-induced and BPDE-induced tail moments were statistically significantly lower in the ever smoker controls than in the never smoker cases (4.43 versus 5.22 for γ-radiation induced tail moment, $P = 0.007$; 2.94 versus 4.59 for γ-radiation induced tail moment, $P < 0.001$).

When the tail moment data were dichotomized at the 75th percentile control value, the higher induced damage was associated with statistically significantly elevated risk for both BPDE-induced damage (OR, 4.49; 95% CI, 2.72-7.42) and γ-radiation-induced damage (OR, 2.32; 95% CI, 1.36-3.95) after adjusting for age, sex, and ethnicity (Table 2).

Lung cancer risk was positively associated with increasing levels of DNA damage across quartiles for both mutagen challenges ($P < 0.001$). For BPDE-induced tail moments, compared with the first quartile, the ORs were 3.96 (95% CIs, 1.64–9.56) for the third quartile and 10.08 (95% CIs, 4.36–23.31) for the fourth quartile. For γ-radiation-induced tail moments, compared with the first quartile, the ORs were 3.48 (95% CIs, 1.62–7.47) for the third quartile and 4.67 (95% CIs, 2.17–10.06) for the fourth quartile.

The median percentage accumulation of cells in γ-radiation-induced S and G_2 arrests was statistically significantly higher in controls than in cases (31.1% versus 22.2% for S phase arrest, $P < 0.001$; 14.9% versus 12.2% for G_2 phase arrest, $P = 0.002$; Fig. 2). When the study subjects were stratified by smoking status and levels of γ-radiation-induced S and G_2 arrests were compared between cases and controls, the median levels of γ-radiation-induced arrest in both the S and G_2 phases were consistently significantly lower in the cases than in the controls, with the exception of γ-radiation-induced G_2 arrest in former smokers, which conformed to the trend but not to statistical significance

Table 2. Association of BPDE- and γ-radiation-induced tail moments with lung cancer risk

Tail moment	Cases (n = 155)	Controls (n = 153)	OR (95% CI)	OR_{adj} (95% CI)*
By 75th percentile value, n (%)				
BPDE				
Low	61 (39.35)	114 (74.51)		
High	94 (60.65)	39 (25.49)	4.50 (2.77–7.32)	4.49 (2.72–7.42)
γ-radiation				
Low	84 (56.76)	108 (75.00)		
High	64 (43.24)	36 (25.00)	2.29 (1.39–3.76)	2.32 (1.36–3.95)
By quartiles, n (%)				
BPDE				
1st quartile	9 (5.81)	39 (25.49)	1.00	1.00
2nd quartile	18 (11.61)	38 (24.84)	2.05 (0.82–5.13)	1.82 (0.72–4.65)
3rd quartile	34 (21.94)	37 (24.18)	3.98 (1.74–9.66)	3.96 (1.64–9.56)
4th quartile	94 (60.64)	39 (25.49)	10.44 (4.62–23.60)	10.08 (4.36–23.31)
P for trend			<0.001	<0.001
γ-radiation				
1st quartile	17 (11.49)	36 (25.00)	1.00	1.00
2nd quartile	21 (14.19)	36 (25.00)	1.24 (0.56–2.72)	1.51 (0.66–3.43)
3rd quartile	46 (31.08)	36 (25.00)	2.71 (1.31–5.58)	3.48 (1.62–7.47)
4th quartile	64 (43.24)	36 (25.00)	3.76 (1.86–7.63)	4.67 (2.17–10.06)
P for trend			<0.001	<0.001

NOTE: BPDE comet data were available for all the 155 cases and 153 controls. γ-Radiation comet data were available for 148 cases and 144 controls.
*Adjusted by age, sex, ethnicity, and smoking status.

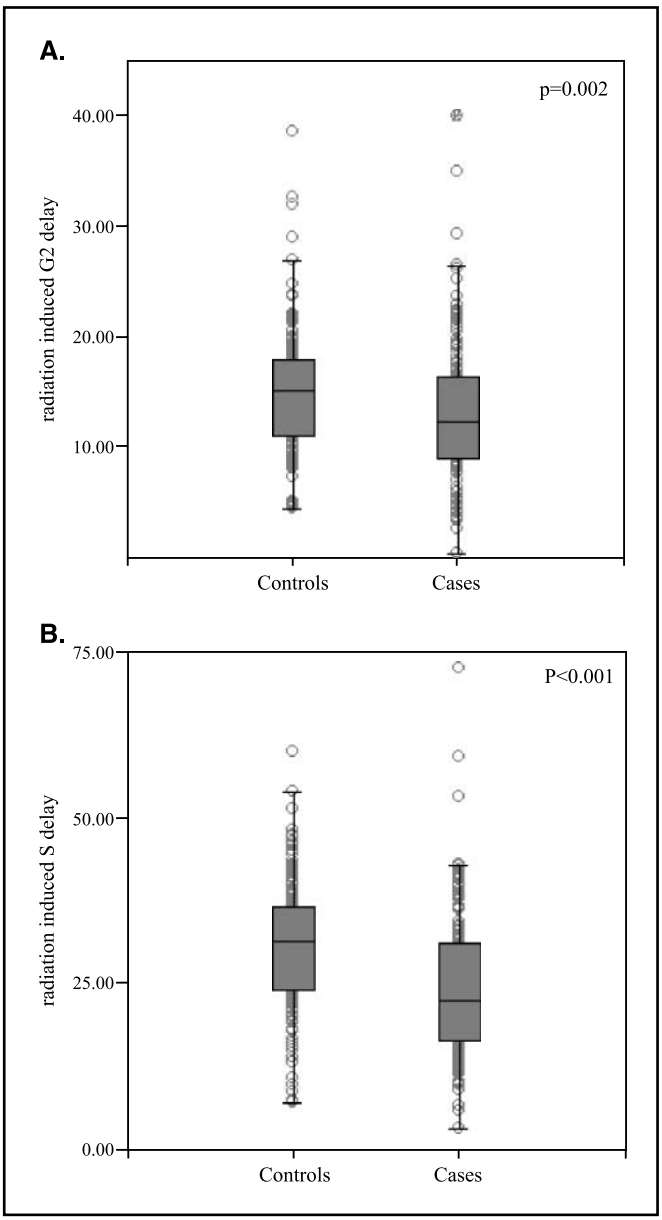

Figure 2. Frequency distribution of γ-radiation-induced G_2 and S phase in lung cancer cases and controls.

(data not shown). When the participants were stratified by case and control status and γ-radiation-induced S and G_2 arrests were compared among never, former, and current smokers, we observed that γ-radiation-induced S and G_2 arrests did not differ by smoking status in either cases or controls (data not shown). We also compared median levels of γ-radiation-induced S and G_2 arrests between ever smoker controls and never smoker cases and discovered that median levels of γ-radiation-induced S and G_2 arrests were statistically significantly higher in ever smoker controls than in never smoker cases (30.5% versus 20.2% for S phase arrest, $P < 0.001$; 15% versus 11.7% for G_2 phase arrest, $P = 0.004$).

Using the 25th percentile value of controls as the cutoff point, the adjusted lung cancer risks were 4.54 (95% CI, 2.70–7.64) for shorter duration of the S phase and 1.85 (95% CI, 1.11–3.08) for shorter duration of the G_2 phase (Table 3). In quartile analysis, significant trends of increasing lung cancer risk were observed as the accumulation of cells in either the S or the G_2 phases decreased. The ORs for the fourth quartile compared with the first quartile were 4.55 (95% CI, 2.30–9.00) for the S phase and 2.11 (95% CI, 1.09–4.08) for the G_2 phase. The Spearman correlation test revealed an inverse correlation between the γ-radiation-induced tail moments and the duration of the S phase ($r = -0.278$, $P = 0.001$) and G_2 phase ($r = -0.159$, $P = 0.057$) and between BPDE-induced tail moments and the duration of the S phase ($r = -0.254$, $P = 0.002$). One additionally significant correlation was observed between the duration of the G_2 and S phases ($r = 392$, $P < 0.001$).

We also stratified the γ-radiation-induced and BPDE-induced tail moments by the duration of the cell cycle delay in both the cases and the control subjects and found that in general, shorter cell cycle delay was associated with higher levels of DNA damage among both the cases and the controls (Table 4). For the S phase, however, only the controls showed statistically significant differences for both mutagens. The median tail moment for a short versus long S phase was 5.18 versus 4.20 ($P = 0.004$) after γ-radiation exposure and 3.05 versus 2.63 ($P = 0.038$) after BPDE exposure. For the G_2 phase, only γ-radiation exposure resulted in statistically significant differences ($P = 0.003$) in the control subjects.

This pattern persisted when the data were categorized by quartile distribution in the control group. With the exception of control BPDE data for the G_2 phase, highest levels of damage were observed in the shortest quartile for both phases. However, the trends were only statistically significant in the controls. Assessing the S phase in controls, the median γ-radiation-induced tail moments were 3.88, 4.46, 4.35, and 5.18 for the longest, 3rd, 2nd, and 1st quartiles, respectively, and the median BPDE-induced tail moments were 2.42, 2.60, 3.08, and 3.05 for the longest, 3rd, 2nd, and 1st quartiles, respectively (P for trend < 0.001).

Furthermore, we assessed the joint effects of S phase arrest and γ-radiation-induced DNA damage in determining lung cancer risk (Table 5). The referent category was individuals with lower levels of damage and longer cell cycle phases. In each instance, highest estimates were evident in the presence of both elevated damage levels and shorter phases. Higher γ-radiation-induced tail moment was associated with a 2-fold increased risk of lung cancer (OR, 2.21; 95% CI, 1.02–4.80); this risk was almost 5-fold for a shorter S phase and low tail moment (OR, 4.86; 95% CI, 2.45–9.63) and 8-fold (OR, 7.52; 95% CI, 3.44–16.41) in those with both a higher γ-radiation-induced tail moment and a shorter S phase. The joint effect of γ-radiation-induced tail moment and shorter G_2 delay resulted in an OR of 3.60, and the joint effect of BPDE-induced tail moment and shorter G_2 delay resulted in an OR of 6.87. In addition, we tested the joint effects between γ-radiation-induced G_2 and S phase duration. Shorter G_2 and longer S phase was not associated with risk of lung cancer (OR 0.64; 95% CI, 0.24–1.72). However, this risk was almost 4-fold for a shorter S and longer G_2 phase (OR, 3.83; 95% CI, 1.91–7.68) and 5-fold (OR, 4.95; 95% CI, 2.55–9.62) in those with both shorter S and shorter G_2 phase. Among all the joint effects, it seemed that the joint effects were more than additive and less than multiplicative interaction except in the joint effects between BPDE-induced tail moment and γ-radiation-induced S phase arrest, which showed more than multiplicative interaction. However, they were not statistically significant.

When the cases were stratified by tumor stage, both early-stage (stages I and II, $n = 33$) and advanced-stage (stages III and IV, $n = 94$)

Table 3. Association of γ-radiation-induced cell cycle G_2 and S phase duration with lung cancer risk

Cell cycle	Cases (n = 155)	Controls (n = 153)	OR (95% CI)	OR_{adj} (95% CI)*
By 25th percentile value, n (%)				
S%†				
Long	66 (42.58)	114 (74.51)		
Short	89 (57.42)	39 (25.49)	3.94 (2.43-6.39)	4.54 (2.70-7.64)
G_2%‡				
Long	96 (61.94)	114 (74.51)		
Short	59 (38.06)	39 (25.49)	1.80 (1.10-2.92)	1.85 (1.11-3.08)
By quartiles, n (%)				
S%†				
4th quartile	22 (14.19)	39 (25.49)	1.00	1.00
3rd quartile	17 (10.97)	38 (24.84)	0.79 (0.37-1.72)	0.78 (0.35-1.75)
2nd quartile	27 (17.42)	37 (24.18)	1.29 (0.63-2.66)	1.24 (0.59-2.61)
1st quartile	89 (57.42)	39 (25.49)	4.05 (2.12-7.70)	4.55 (2.30-9.00)
P for trend			<0.001	<0.001
G_2%‡				
4th quartile	30 (19.35)	37 (24.18)	1.00	1.00
3rd quartile	21 (13.55)	38 (24.84)	0.68 (0.33-1.40)	0.76 (0.36-1.58)
2nd quartile	45 (29.03)	39 (25.49)	1.42 (0.75-2.71)	1.66 (0.85-3.25)
1st quartile	59 (38.06)	39 (25.49)	1.87 (0.99-3.50)	2.11 (1.09-4.08)
P for trend			0.010	0.005

*Adjusted by age, sex, ethnicity, and smoking status.
†Percentage of cells in S phase after γ-radiation.
‡Percentage of cells in G_2 phase after γ-radiation.

cases had statistically higher γ-radiation-induced tail moments than controls; however, no difference was found between the early- and advanced-stage cases (5.02 versus 5.62, P = 0.126). On the other hand, patients with advanced lung cancer exhibited higher BPDE-induced tail moments compared with patients with early disease stage (4.43 versus 2.95, P = 0.021). The advanced-stage cases exhibited higher BPDE-induced tail moments than controls. Similar trend was also observed for early-stage cases, although it did not reach statistical significance (P = 0.253). Finally, when the cases were stratified by tumor stages, both early- and advanced-stage cases had statistically lower γ-radiation-induced S and G_2 arrests than controls, but no difference was observed between the early- and advanced-stage cases (S delay: 25.9% versus 22.4%, P = 0.321; G_2 delay: 12.8% versus 12.6%, P = 0.442).

In terms of histology type, 83 patients had adenocarcinoma, 34 patients had squamous cell carcinoma, 22 patients had non–small-cell carcinoma, 9 patients had large cell carcinoma, and 5 patients had other types of carcinoma. There was no statistically significant difference among histologic types in terms of both γ-radiation- and BPDE induced tail moments and γ-radiation-induced S and G_2 phase (data not shown).

Discussion

In this case-control lung cancer study, we used the comet assay to measure mutagen-induced DNA damage and the FACS to measure cell cycle checkpoints. The main finding of this study was that peripheral blood lymphocytes from patients with lung cancer exhibited higher levels of mutagen-induced DNA damage than those from controls. Furthermore, patients with lung cancer exhibited significantly shorter cell cycle delays in response to an *in vitro* mutagen challenge. In addition, we observed joint effects between levels of DNA damage and deficient cell cycle checkpoints on lung cancer risk, a trend of increasing risk with increasing levels of genetic damage, a trend of increasing risk with decreasing accumulation of cells in either the S or the G_2 phases, and significant correlation between these two damage checkpoint measurements.

Our results are consistent with other recent studies on DNA repair capacity. Hsu et al. (20) have suggested that environmentally induced genetic damage accumulates more rapidly in people with suboptimal DNA repair capacity than in similarly exposed people without such defects. Commensurate with this hypothesis, both *in vitro* and *in vivo* studies have shown that defects in the DNA repair system are related to hypersensitivity to carcinogen exposure in Nijmegen breakage syndrome and ataxia-telangiectasia cells and in ligase-deficient mice (21, 22). Xeroderma pigmentosum cell lines that are defective in their nucleotide excision repair capabilities exhibit higher numbers of BPDE-induced chromosome breaks compared with normal cell lines (3). Clinically, patients with the Nijmegen breakage syndrome have a defect in homologous recombination and are hypersensitive to radiation (23).

We observed that the median duration of the γ-radiation-induced S phase was statistically significantly longer in the controls than in the cases and that a shorter γ-radiation-induced S phase was associated with a 4-fold increased risk of lung cancer. It has

been shown that the S-phase checkpoint is deficient in responding to ionizing radiation in people with ataxia-telangiectasia syndrome and Nijmegen breakage syndrome (24, 25), as well as in cancer patients with mutations in the *CHK1* gene (26). We also found that the median duration of the γ-radiation-induced G_2 phase was significantly higher in controls than in cases and that a shorter γ-radiation-induced G_2 phase was associated with a 2-fold elevated risk of lung cancer. This finding is corroborated by our previous study of lymphoblastoid cell lines (19) and Olivieri and Micheli's conclusion that when G_2 arrest did not occur after irradiation, the daughter cells displayed the highest level of induced chromosome aberrations (27). Piette and Munoz (28) showed that defects in the G_2 phase arrest was strongly related to human carcinogenesis and that the signaling pathway that leads to G_2 arrest is often altered in human cancer (12). Therefore, individuals with defects in the G_2 phase checkpoints may be predisposed to lung cancer.

In addition, we found that mutagen-induced damage was greater in both cases and controls with shorter S and G_2 phases. This finding is best explained by the types of repair pathways elicited by different mutagens in damage response, as well as by the dual role of p53 in DNA repair and cell cycle control. In an illustration of the role of p53 in DNA repair, BPDE-induced DNA damage elicits the nucleotide excision repair pathway, which has also been shown to be regulated by p53: cells lacking functional p53 have shown both greater susceptibility to and defective repair of UV-induced DNA damage, which triggers nucleotide excision repair (29–35). Much stronger is the evidence for a direct role for the p53 protein in base excision repair because γ-radiation induces base excision repair, which is also regulated by p53. Conversely, base excision repair is deficient in p53-null cells (36, 37). Further evidence for the direct role of p53 in base excision repair comes from the fact that p53 directly interacts with DNA polymerase β and stabilizes the interaction between DNA polymerase and abasic DNA. Furthermore, transactivation-defective N-terminal mutant forms of p53 do not interact with DNA polymerase β and cannot stimulate base excision repair (37).

Our findings support our hypothesis that individuals with defects in both cell cycle checkpoint and DNA repair capacity would have significantly elevated cancer risks compared with individuals with a defect in only one pathway. Specifically, we found that the risks associated with both shorter G_2 phase and elevated DNA damage were substantially increased. Similarly, joint effects were observed for a shorter S phase. Biologically, therefore, cell cycle control and the DNA repair capacity constitute two distinct but interrelated cellular pathways that modulate cellular responses to carcinogen exposure and, thus, cancer risk.

Table 4. Tail moment distribution stratified by duration of cell cycle delay

Cell cycle checkpoints	Cases				Controls			
	n	γ-Radiation, tail moment median (range)	*n*	BPDE, tail moment median (range)	*n*	γ-Radiation, tail moment median (range)	*n*	BPDE, tail moment median (range)
S%*								
By 25th percentile value								
Long	62	5.15 (1.60-9.63)	66	3.99 (1.60-8.04)	107	4.20 (1.50-10.48)	114	2.63 (1.27-8.46)
Short	86	5.59 (1.82-11.39)	89	4.37 (1.50-9.13)	37	5.18 (1.84-10.15)	39	3.05 (1.03-8.44)
P		0.289		0.113		0.004		0.038
By quartiles								
4th quartile	20	5.50 (2.62-7.71)	22	4.69 (1.81-7.48)	36	3.88 (1.50-10.48)	39	2.42 (1.50-8.46)
3rd quartile	17	4.91 (1.60-9.51)	17	3.59 (1.68-7.20)	37	4.46 (1.55-7.54)	38	2.60 (1.27-8.06)
2nd quartile	25	5.10 (2.42-9.63)	27	3.51 (1.60-8.04)	34	4.35 (1.93-9.68)	37	3.08 (1.33-6.43)
1st quartile	86	5.59 (1.82-11.39)	89	4.37 (1.50-9.13)	37	5.18 (1.84-10.15)	39	3.05 (1.03-8.44)
P for trend		0.51		0.63		<0.001		<0.001
G_2%†								
By 25th percentile value								
Long	91	5.25 (1.60-9.74)	96	3.99(1.60-8.47)	108	4.17 (1.50-10.48)	114	2.75 (1.27-8.46)
Short	57	5.36 (2.18-11.39)	59	4.37(1.50-9.13)	36	5.28 (2.76-8.12)	39	2.92 (1.03-8.27)
P		0.432		0.237		0.003		0.293
By quartiles								
4th quartile	29	5.10 (2.62-8.33)	30	3.91 (1.60-8.04)	33	3.81 (2.23-10.48)	37	2.86 (1.47-8.44)
3rd quartile	20	5.45 (1.60-9.63)	21	4.22 (1.68-8.36)	36	4.17 (1.50-10.15)	38	2.54 (1.27-5.60)
2nd quartile	42	5.40 (1.82-9.74)	45	3.99 (1.81-8.47)	39	4.35 (1.55-10.11)	39	3.17 (1.33-8.46)
1st quartile	57	5.36 (2.18-11.39)	59	4.37 (1.50-9.13)	36	5.28 (2.76-8.12)	39	2.92 (1.03-8.27)
P for trend		0.38		0.30		0.02		0.13

*Percentage of cells in S phase after γ-radiation.
†Percentage of cells inG_2 phase after γ-radiation.

Table 5. Joint effects of cell cycle checkpoints and DNA damage in lung cancer risk

Tail moment	γ-Radiation-induced S-phase arrest*			
	Long		Short	
	Case/control, *n*	ORs (95% CI)†	Case/control, *n*	ORs (95% CI)†
γ-Radiation induced				
Low	40/87	1.00	44/21	4.86 (2.45–9.63)
High	22/20	2.21 (1.02–4.80)	42/16	7.52 (3.44–16.41)
BPDE induced				
Low	30/86	1.00	31/28	3.63 (1.77–7.45)
High	36/28	3.47 (1.77–6.80)	58/11	20.77 (8.65–49.90)
	γ-Radiation-induced G_2-phase arrest‡			
	Long		Short	
	Case/control, *n*	ORs (95% CI)†	Case/control, *n*	ORs (95% CI)†
γ-Radiation induced				
Low	53/86	1.00	31/22	2.20 (1.12–4.33)
High	38/22	2.59 (1.31–5.09)	26/14	3.60 (1.61–8.01)
BPDE induced				
Low	40/88	1.00	21/26	1.91 (0.92–4.00)
High	56/26	4.63 (2.49–8.62)	58/11	6.87 (3.15–14.99)

*Percentage of cells in S phase after γ-radiation.
†Adjusted by age, sex, ethnicity, and smoking status.
‡Percentage of cells in G_2 phase after γ-radiation.

To our knowledge, this is the first molecular epidemiologic study to investigate the association between both cell cycle checkpoints and DNA damage/repair capacity in determining lung cancer risk. Our data show that deficiencies in cell cycle checkpoints and DNA damage/repair capacity contribute independently and jointly to elevated lung cancer risk.

Acknowledgments

Received 4/14/2004; revised 9/10/2004; accepted 10/27/2004.

Grant support: Grants CA 55769, CA 68437, CA86390, and CA 74880.

The costs of publication of this article were defrayed in part by the payment of page charges. This article must therefore be hereby marked advertisement in accordance with 18 U.S.C. Section 1734 solely to indicate this fact.

We thank Dr. Kim-Anh Do and Marcella M. Johnson for statistical consultations.

References

1. Rouse J, Jackson SP. Interfaces between the detection, signaling, and repair of DNA damage. Science 2002; 297:547–51.
2. Berwick M, Vineis P. Markers of DNA repair and susceptibility to cancer in humans: an epidemiologic review. J Natl Cancer Inst 2000;92:874–97.
3. Wu X, Gu J, Hong WK, et al. Benzo[*a*]pyrene diol epoxide and bleomycin sensitivity and susceptibility to cancer of upper aerodigestive tract. J Natl Cancer Inst 1998;90:1393–9.
4. Wei Q, Cheng L, Amos CI, et al. Repair of tobacco carcinogen-induced DNA adducts and lung cancer risk: a molecular epidemiologic study. J Natl Cancer Inst 2000;92:1764–72.
5. Wei Q, Spitz MR, Gu J, et al. DNA repair capacity correlates with mutagen sensitivity in lymphoblastoid cell lines. Cancer Epidemiol Biomarkers Prev 1996;5:199–204.
6. Singh NP, Stephens RE. Microgel electrophoresis: sensitivity, mechanisms, and DNA electrostretching. Mutat Res 1997;383:167–75.
7. Rajeswari N, Ahuja YR, Malini U, et al. Risk assessment in first degree female relatives of breast cancer patients using the alkaline comet assay. Carcinogenesis 2000; 21:557–61.
8. Colleu-Durel S, Guitton N, Nourgalieva K, Leveque J, Danic B, Chenal C. Genomic instability and breast cancer. Oncol Rep 2001;8:1001–5.
9. Rajaee-Behbahani N, Schmezer P, Risch A, et al. Altered DNA repair capacity and bleomycin sensitivity as risk markers for non-small cell lung cancer. Int J Cancer 2001;95:86–91.
10. Kleinsasser NH, Wagner C, Wallner BC, Harreus UA, Kastenbauer ER. Mutagen sensitivity of nasopharyngeal cancer patients. Mutat Res 2001;491:151–61.
11. Bartek J, Lukas J. Mammalian G_1 and S phase checkpoints in response to DNA damage. Curr Opin Cell Biol 2001;13:738–47.
12. Molinari M. Cell cycle checkpoints and their inactivation in human cancer. Cell Prolif 2000;33:261–74.
13. Shiloh Y. Ataxia-telangiectasia and the Nijmegen breakage syndrome: related disorders but genes apart. Annu Rev Genet 1997;31:635–62.
14. Hudmon KS, Honn SE, Jiang H, et al. Identifying and recruiting healthy control subjects from a managed care organization: a methodology for molecular epidemiological case-control studies of cancer. Cancer Epidemiol Biomarkers Prev 1997;6:565–71.
15. Schabath MB, Spitz MR, Grossman HB, et al. Genetic instability in bladder cancer measured by the comet assay. J Natl Cancer Inst 2003;95:540–7.
16. Singh NP, McCoy MT, Tice RR, Schneider EL. A simple technique for quantitation of low levels of DNA damage in individual cells. Exp Cell Res 1988;175: 184–9.
17. Pandita TK, Hittelman WN. The contribution of DNA and chromosome repair deficiencies to the radiosensitivity of ataxia-telangiectasia. Radiat Res 1992;131:214–23.
18. Olive PL, Banath JP, Durand RE. Heterogeneity in radiation-induced DNA damage and repair in tumor and normal cells measured using the "comet" assay. Radiat Res 1990;122:86–94.
19. Zhao H, Spitz MR, Tomlinson GE, Zhang H, Minna JD, Wu X. γ-Radiation-induced G_2 delay, apoptosis, and p53 response as potential susceptibility markers for lung cancer. Cancer Res 2001;61:7819–24.
20. Hsu TC, Johnston DA, Cherry LM, et al. Sensitivity to genotoxic effects of bleomycin in humans: possible relationship to environmental carcinogenesis. Int J Cancer 1989;43:403–9.
21. Little JB, Nagasawa H, Dahlberg WK, Zdzienicka MZ, Burma S, Chen DJ. Differing responses of Nijmegen breakage syndrome and ataxia telangiectasia cells to ionizing radiation. Radiat Res 2002;158:319–26.
22. Harrison C, Ketchen AM, Redhead NJ, O'Sullivan MJ, Melton DW. Replication failure, genome instability, and increased cancer susceptibility in mice with a point

mutation in the DNA ligase I gene. Cancer Res 2002; 62:4065–74.
23. van der Burgt I, Chrzanowska KH, Smeets D, Weemaes C. Nijmegen breakage syndrome. J Med Genet 1996;33:153–6.
24. Xu B, O'Donnell AH, Kim ST, Kastan MB. Phosphorylation of serine 1387 in Brca1 is specifically required for the Atm-mediated S-phase checkpoint after ionizing irradiation. Cancer Res 2002;62:4588–91.
25. Girard PM, Riballo E, Begg AC, Waugh A, Jeggo PA. Nbs1 promotes ATM dependent phosphorylation events including those required for G_1/S arrest. Oncogene 2002;21:4191–9.
26. Feijoo C, Hall-Jackson C, Wu R, et al. Activation of mammalian Chk1 during DNA replication arrest: a role for Chk1 in the intra-S phase checkpoint monitoring replication origin firing. J Cell Biol 2001;154:913–23.
27. Olivieri G, Micheli A. Mitotic delay and repair in human lymphocytes. Mutat Res 1983;122:65–72.
28. Piette J, Munoz P. Implication of the G_2 checkpoint in the maintenance of genome integrity. Pathol Biol (Paris) 2000;48:174–81.
29. Smith ML, Chen IT, Zhan Q, O'Connor PM, Fornace AJ Jr. Involvement of the p53 tumor suppressor in repair of UV-type DNA damage. Oncogene 1995;10:1053–9.
30. Ford JM, Hanawalt PC. Li-Fraumeni syndrome fibroblasts homozygous for p53 mutations are deficient in global DNA repair but exhibit normal transcription-coupled repair and enhanced UV-resistance. Proc Natl Acad Sci U S A 1995;92:8876–80.
31. Havre PA, Yuan J, Hedrick L, Cho KR, Glazer PM. P53 inactivation by HPV16-E6 results in increased mutagenesis in human cells. Cancer Res 1995;55:4420–4.
32. Ford JM, Baron EL, Hanawalt PC. Human fibroblasts expressing the human papillomavirus E6 gene are deficient in global genomic nucleotide excision repair and sensitive to UV-irradiation. Cancer Res 1998;58: 599–603.
33. Cistulli CA, Kaufmann WK. p53-dependent signalling sustains DNA replication and enhances clonogenic survival in 254 nm ultraviolet-irradiated human fibroblasts. Cancer Res 1998;58:1993–2002.
34. El-Mahdy MA, Hamada PM, Wani MA, Zhu Q, Wani AA. P53 degradation by HPV16-E6 preferentially affects the removal of cyclobutane pyrimidine dimers from non-transcribed strand and sensitizes mammary epithelial cells to UV-irradiation. Mutat Res 2000;459: 135–45.
35. McKay BC, Chen F, Perumalswami CR, Zhang F, Ljungman M. The tumor suppressor p53 can both stimulate and inhibit ultraviolet-light-induced apoptosis. Mol Biol Cell 2000;11:2543–51.
36. Offer H, Zurer I, Banfalvi G, et al. P53 modulates base excision repair activity in cell cycle specific manner after genotoxic stress. Cancer Res 2001;61:88–96.
37. Zhou J, Ahn J, Wilson SH, Prives C. A role for p53 in base excision repair. EMBO J 2001;20:914–23.